Computer Simulation of the Ion Escape from High-Energy Electron Tracks in Nonpolar Liquids

Laurens D. A. Siebbeles,*,† Witold M. Bartczak,†,‡ Michel Terrissol,§ and Andries Hummel†

Interfaculty Reactor Institute, Mekelweg 15, 2629 JB Delft, The Netherlands, Institute of Applied Radiation Chemistry, Technical University, Lodz, Poland, and CPAT, Université Paul Sabatier, Toulouse, France

Received: July 17, 1996; In Final Form: November 7, 1996[⊗]

The number of ions escaping from recombination in high-energy electron tracks in saturated hydrocarbon liquids is calculated and compared with experimental results from the literature. The initial track structure is obtained by bringing the details of the electron scattering into account. The number of positive ions and electrons that escape from charge recombination is obtained from a computer simulation of the trajectories of the positive ions and the electrons. The probability that the charges escape from each other is seen to change appreciably with the energy of the primary high-energy electron. The thermalization distance distribution of the electrons in the track is obtained by comparing the calculated results with those from experiments. The influence of external electric fields on the escape of ions is considered.

I. Introduction

A high-energy charged particle causes ionizations and electronic excitations along its path through a medium. The secondary electrons that are produced with sufficient energy will cause further ionizations and excitations until they become thermalized. In this way, a track of positive ions, thermalized electrons, and electronically excited molecules is formed. The reactions of these transients eventually give rise to the chemical effects of high-energy radiation. The nonhomogeneous kinetics of the reactions of the transients in charged particle tracks has received considerable attention through the years.[1−6]

In nonpolar liquids, the Coulomb forces between the ions in the track extend over large distances, resulting in significant interactions between many ions. This complicates the nonhomogeneous kinetics for the ions in contrast to that for neutral species or ions in high-permittivity liquids like water, where the Coulomb forces are small and theoretical methods are advanced. The positive ions and electrons in the track in a nonpolar liquid move due to diffusion and drift in each other's Coulomb field and can either recombine or escape from each other. The present work concerns computer simulations of the dynamics of the charged species in the tracks in the presence and absence of an external electric field, in order to calculate the number of ions that escape from a high-energy electron track in a nonpolar liquid. Several experimental studies have been concerned with the determination of the number of escaped ions from high-energy electron tracks.[7−10] It is the aim of this work to obtain information about the initial configuration of the positive ions and electrons in the tracks by a comparison of calculated and experimental results. In particular, the determination of the electron thermalization distribution will be considered, which thus far could only be carried out in a very approximate fashion.

Computer calculations of the kinetics of the reactions in groups of transient species, using the so-called independent pairs approximation,[11] have been presented. This approximation has been applied to small groups of ions in both high- and low-permittivity liquids,[5,6,11−16] and the results have been compared to those obtained by full Monte Carlo simulations of the paths of the species. For tracks containing many interacting species, a full Monte Carlo simulation of the trajectories of the species is needed to study their kinetics.

Computer calculations on the escape of ions in nonpolar liquids have been performed previously[17] with cylindrical model electron tracks, using the method of ref 18 to simulate the motion of the ions due to diffusion and drift in each other's Coulomb field. In the present work, this method is applied to electron tracks where the positions of the ionizations were calculated by bringing the details of the scattering of the incoming electron into account.

If the primary electron has a sufficiently high energy, the energy losses will occur at sites well separated from each other and the track consists of independent tracks of secondary electrons with lower energies. The number of escaped ions from a high-energy electron track can then be obtained by adding the results for the tracks of the secondary electrons with lower energies. While in the work of ref 17 experimental gas-phase distributions were used for the number of ions produced by the low-energy losses of the primary electron, in the present work, the relativistic Bethe theory for electron scattering is used to describe the low-energy-loss distribution. Since the calculated results are compared with those from experiments, which have been conducted in the presence of an external electric field, the influence of external electric fields on the escape of ions from a track is also addressed.

Throughout this work, the escape of ions will be expressed in terms of the radiation chemical yield, which is defined as the number of escaped ion pairs per 100 eV of energy absorbed by the medium. Thus, if $N_{esc}(E)$ ion pairs escape from a track of an incoming electron with an energy E (in eV), the ion escape yield is equal to $G_{esc}(E) = 100N_{esc}(E)/E$. The probability for an ion pair to escape from a track is defined as $p_{esc}(E) = G_{esc}(E)/G_0(E) = N_{esc}(E)/N_0(E)$, where $G_0(E)$ is the initial ion yield and $N_0(E)$ is the total initial number of ion pairs.

The method by which the electron tracks are calculated and the method used to calculate the ion escape yield are discussed in section II. In section III, the calculated ion escape yields

* E-mail: SIEBBEL@IRI.TUDELFT.NL. FAX: ++31 15 27 87 42 1.
† Interfaculty Reactor Institute.
‡ Institute of Applied Radiation Chemistry.
§ CPAT.
⊗ Abstract published in *Advance ACS Abstracts,* January 15, 1997.

S1089-5639(96)02166-4 CCC: $14.00

are discussed and compared with experimental results from the literature. A summary and our conclusions are presented in section IV.

II. Computational Section

A. Initial Spatial Distribution of Positive Ions and Thermalized Electrons in an Electron Track. The spatial distributions of the positive ions in tracks of electrons with initial kinetic energies, E, between 40 eV and 30 keV were calculated by Monte Carlo simulations, as described in ref 19. To perform these simulations, the characteristics of the electron scattering in the medium must be known. The scattering processes that were considered in the simulation of an electron track are inelastic scattering due to excitation of a valence or inner-shell electron and elastic scattering. Excitation of an electron in the medium can lead to ionization, and in that case, a secondary electron is produced. This secondary electron can then cause further ionizations if it has sufficient energy. The trajectory of a primary or secondary, etc., electron was calculated until it had reached an energy of less than 20 eV. The probability distribution of the path length, l, of an electron between successive scattering events was taken to be $f(l) = l_{av}^{-1} \exp(-l/l_{av})$. The mean free path, $l_{av} = (\sum_i N_i \sigma_i(E))^{-1}$, is determined by the number densities, N_i, of the scattering centers in the medium and by the scattering cross sections, $\sigma_i(E)$. After a step in the trajectory of the primary electron, the probability for a scattering event of type j is equal to $P_j = N_j\sigma_j(E)/[\sum_i N_i\sigma_i(E)]$. In the case of inelastic scattering, the probability for an energy transfer, E', from the primary to the secondary electron is $\sigma_j(E,E')/\sigma_j(E)$, with $\sigma_j(E) = \int \sigma_j(E,E')\mathrm{d}E'$.

The differential cross section, $\sigma(E,E')$, for excitation of the valence electrons was obtained from the work of Ashley et al.[20,21] In this work, the cross section is obtained by integration of the energy-loss function, $\mathrm{Im}\{-1/\epsilon(q,E')\}$ (the imaginary part of the negative reciprocal of the complex dielectric response function of the medium), over all possible momentum transfers, q. The energy-loss function, $\mathrm{Im}\{-1/\epsilon(q,E')\}$, for non-zero momentum transfer is obtained from the optical energy-loss function ($q = 0$). The optical energy-loss function is related to the dipole oscillator strength distribution.[22,23] As has been shown in the recent work of LaVerne and Pimblott, the dipole oscillator strength distributions of gaseous hydrocarbons differ significantly from those in the condensed phase.[24] However, the dipole oscillator strength distributions are very similar for different solid hydrocarbons and do not change very much when going from the solid to the liquid phase.[24] The dipole oscillator strength distribution of polyethylene obtained from the work of Painter et al.[25] (by using the relation between the oscillator strength and the energy-loss function, see eq 7 in section II.C) does not differ substantially from that of the solid hydrocarbons (e.g., cyclohexane, cyclohexene, cyclohexadienes) presented in ref 24 and is therefore considered to be representative of saturated hydrocarbon liquids. The scattering angle of an electron after excitation of a valence electron was obtained from the angular distribution for scattering of electrons in a Fermi electron gas, as described in ref 26.

To calculate the probability for excitation of the inner-shell electrons, the total cross section of Gryzinsky[27] was used. The energy-loss distribution was obtained from the differential electron scattering cross section, $\sigma(E,E')$, of Mott,[28,29] which is equal to the nonrelativistic limit of the Møller cross section.[30] For these knock-on collisions, the scattering angles of the incident and ejected electron were calculated by means of classical mechanics. After excitation of an inner-shell electron had occurred, the excited singly charged positive ion was assumed to decay by fluorescence or via an Auger process, leading to the production of a doubly charged positive ion and two secondary electrons. The yield of fluorescence for inner-shell excitation of a carbon atom was taken from the work of Scofield.[31]

The elastic scattering of the electrons was taken into account by using the model of Massey, in which the amplitude for scattering of an electron by a molecule is written as a coherent sum of amplitudes for scattering by the constituent atoms.[32] The molecular unit onto which scattering occurs in polyethylene was taken to be C_3H_6. The phase shifts in the scattered amplitudes were calculated by using the electron−atom potentials for carbon and hydrogen atoms, which were written as a sum of Yukawa potentials with parameters given by Cox and Bonham.[33]

Since the mean free path for electron scattering is inversely proportional to the electron density, the initial track structures in the hydrocarbon liquids were obtained by scaling the coordinates of the scattering positions in a track, as calculated for polyethylene, with the relative density of the hydrocarbon liquids. The density used in the calculations of the tracks in polyethylene was 0.9 g/cm^3; for the hydrocarbon liquids to be considered below, the density is close to 0.7 g/cm^3. Therefore, the coordinates of the scattering positions as calculated for polyethylene were multiplied by a factor of 0.9/0.7, unless stated otherwise. However, if this scaling factor was not brought into account, the calculated escape yields were found not to differ appreciably.

To determine the kinetic energy of the secondary electrons after excitation by the incoming electron, the binding energies of the electrons in the medium must be known. The valence electrons in polyethylene (the carbon $n = 2$ electrons and the hydrogen 1s electrons) were treated as a free electron gas at absolute zero temperature.[34] The density of states, ρ, for electrons with an energy I below the Fermi level is then $\rho(I) = {}^3/_2 E_F^{-3/2}(E_F - I)^{1/2}$. The Fermi energy is equal to $E_F = (\hbar^2/(2m_e))(3\pi^2 n_v)^{2/3}$, with n_v being the number density of the valence electrons with mass m_e and $\hbar$ being Planck's constant divided by 2π. The Fermi energy for polyethylene with a mass density of 0.9 g/cm^3 is then calculated to be $E_F = 13.8$ eV. The binding energy of the inner-shell 1s electrons of the carbon atoms was taken to be 284 eV below the Fermi energy.

An energy loss, E', from an incoming electron to an electron in the medium with binding energy I gives a secondary electron with an energy $E_{el} = E' - I$ above the Fermi level. The concept of ionization in the condensed phase is complicated. It is not known to which extent excitation of an electron to a certain energy E_{el} above the Fermi level is to be treated as an ionization, i.e., gives a positive ion and an electron that move due to diffusion and drift in each other's Coulomb field. If all excitations of electrons, irrespective of the value of E_{el}, are assumed to correspond to an ionization, the initial ion yield in the tracks was calculated to be $G_0 = 5.9(100\ \mathrm{eV})^{-1} \pm 4\%$. In gaseous hydrocarbons, the initial ion yield is around $4(100\ \mathrm{eV})^{-1}$ [35] and is estimated to be somewhat larger in the liquid phase.[36] A value of $G_0 = 5.9(100\ \mathrm{eV})^{-1}$ is considered somewhat high, and therefore, in most of the calculations discussed below, ionization was assumed to occur for energies E_{el} larger than 3.2 eV, giving $G_0 = 5.0(100\ \mathrm{eV})^{-1} \pm 4\%$. The effect of the initial ion yield, G_0, on the results will be discussed below.

It was assumed that electrons with an energy below 20 eV cannot cause ionizations. This assumption introduces another uncertainty in the initial ion yield. The position at which an electron with an energy below 20 eV reaches thermal energy cannot be calculated, due to the lack of appropriate cross-

sectional data. Therefore, the distribution of distances from the positive ion at which the secondary electron becomes thermalized, the thermalization distance distribution, is assumed adjustable. It is one of the aims of this work to determine this distribution by comparing calculated and experimental results. It was assumed that the secondary electrons thermalize symmetrically around the positive ions. Calculations are performed for exponential and Gaussian distributions given by

$$f_{\mathrm{exp}}(r)\,\mathrm{d}r = \frac{1}{r_{\mathrm{av}} - r_{\mathrm{reac}}} \mathrm{e}^{-(r-r_{\mathrm{reac}})/(r_{\mathrm{av}}-r_{\mathrm{reac}})}\,\mathrm{d}r \qquad \text{for} \quad r > r_{\mathrm{reac}}$$

$$f_{\mathrm{exp}}(r)\,\mathrm{d}r = 0 \qquad \text{for} \quad r \le r_{\mathrm{reac}} \tag{1a}$$

and

$$f_{\mathrm{Gauss}}(r)\,\mathrm{d}r = \frac{32r^2}{\pi {r_{\mathrm{av}}}^3} \mathrm{e}^{-4r^2/(\pi {r_{\mathrm{av}}}^2)}\,\mathrm{d}r \tag{1b}$$

In eq 1, r is the distance between the electron and the positive ion around which the electron has become thermalized, r_{av} is the average thermalization distance, and r_{reac} is the reaction radius at which recombination of opposite charges occurs (see section II.B).

If the primary electron is produced by a high-energy photon, there is a positive ion at the origin of the electron track and the primary electron becomes thermalized at a position far away from its parent positive ion. Also, secondary electrons with energies large enough to cause further ionizations will not thermalize around their parent positive ion. In the calculations of this work, a thermalized electron is taken around each positive ion in the track. In order to investigate the effect of this simplification, simulations (by the method of section II.B) were also performed by taking the position where the secondary electrons have an energy below 20 eV as the position around which thermalization occurs. The ion escape yields, obtained from these simulations (with a Gaussian distribution with $r_{\mathrm{av}} = 12$ nm, see eq 1b), did not show a deviation larger than 5% compared to the simulation assuming thermalization around the positive ion positions.

B. Ion Escape from Tracks of Electrons with Energies up to 30 keV. After the initial spatial distribution of the positive ions and thermalized electrons had been calculated, a computer simulation of the motion of the charges was performed in order to obtain the ion escape yield. The computer simulation method has been published elsewhere[18] and is therefore only briefly described here. The displacement $\delta \mathrm{r}_i$ of a charged particle during a small time step δt was calculated according to

$$\delta \mathbf{r}_i = \mu_i \mathbf{E}_i \delta t + (6 D_i \delta t)^{1/2} \mathbf{R}_i \tag{2}$$

The first term in eq 2 represents the drift of the particle in the electric field, $\mathbf{E}_i$, due to the Coulomb interactions with all the other particles and the interaction with a possible external electric field. The mobility of the particle is denoted by μ_i and is related to the diffusion coefficient, D_i, by $\mu_i = eD_i/kT$, with e the charge of an electron, k the Boltzmann constant, and T the absolute temperature. The second term in eq 2 describes the motion due to random diffusion. The random vector $\mathbf{R}_i$ has a uniformly distributed orientation and a uniformly distributed length, chosen such that $\langle \mathbf{R}_i^2 \rangle = 1$. Recombination of opposite charges was assumed to occur if the distance between a positive ion and an electron became smaller than the reaction radius, r_{reac}, which was taken to be 15 Å.

The simulations were continued until one ion pair remained or until a time limit was reached. If one ion pair remained, the ion escape yield was calculated by application of the Onsager formula[37] for the escape probability of the last pair $P_{\mathrm{esc}} = \exp(-r_{\mathrm{c}}/r)$, with the Onsager distance $r_{\mathrm{c}} = e^2/(4\pi\epsilon_0\epsilon_{\mathrm{r}}kT)$, where ϵ_0 is the permittivity of vacuum and ϵ_{r} the relative permittivity of the medium. If more than one ion pair was left after a time equal to $10^3 {r_{\mathrm{c}}}^2/(D_+ + D_-)$ (with D_+ and D_- being the diffusion coefficients of the positive ion and the electron), the escape yield was calculated from the Onsager escape probabilities for the ion pair with the smallest distance between the positive ion and the electron, then for the next but smallest and so forth. In all cases, where more than one ion pair was left at the end of the simulation, the number of escaping ions calculated in this way was at most 2% smaller than the actual number of ion pairs left, indicating that all electrons and ions were well separated at the end of the simulations.

For each electron track, several simulations of the motion of the charged species were performed, using different initial positions of the electrons sampled from the distribution in eq 1a or eq 1b (and different random vectors $\mathbf{R}_i$ in eq 2). For each energy of the primary electron, this was carried out for 10 different track structures. The statistical error in the final averaged escape yields is estimated to be less than 5%.

The diffusion coefficients were taken to be $D_+ = D_- = 1.264 \times 10^{-9}$ m^2/s, which at $T = 293$ K gives a value for $\mu_+ = \mu_- = 5 \times 10^{-8}$ m^2/(V s). The relative dielectric constant was taken to be $\epsilon_{\mathrm{r}} = 2$. The diffusion coefficients of the electrons in the hydrocarbon liquids used in the experimental studies to be discussed in section III differ by about 2 orders of magnitude. This raises the question as to which extent the ion escape yield is affected by the diffusion coefficients of the charged particles. The Onsager formula for ion escape from a single pair does not depend on the magnitude of the diffusion coefficients. It was found that changing the diffusion coefficients for either the positive ion, the electron, or both by 3 orders of magnitude did not change the calculated escape yield from tracks of electrons with energies from 40 eV up to 2 keV by more than the statistical error in the calculations. Deviations do occur for very long mean free paths for electron scattering, as has been shown in refs 38−42. However, preliminary results have shown that for the cases considered here, this effect is negligible.[43]

C. Ion Escape from Tracks of Electrons with Energies above 30 keV. For larger energies of the primary electron, the energy losses occur at larger distances from each other. For sufficiently high energies of the primary electron, the losses will occur spaced widely enough so that the secondary electron tracks due to subsequent losses do not overlap and interactions between species in different secondary electron tracks become negligible. In that case, the total yield of ion escape from the primary electron track will, to a good approximation, be determined by the yields from the individual tracks of the secondary electrons.

For large energies of the primary electron, the ion escape yield is obtained from the yields from tracks with lower energies, by using a method analogous to that presented by Magee and Chatterjee.[44] The present treatment differs from that of ref 44 by the fact that no division is made between energy losses below and above 100 eV. In the work of ref 44 the contribution to the yield by all energy losses below 100 eV was brought into account by assuming a value for the yield due to these low losses. In this work, the yields for the small energy losses are obtained from the simulations as described in sections II.A and II.B.

For energy losses close to the binding energy of an electron in the medium, the kinetic energy of the secondary electron will be significantly smaller than the energy loss. Since the

number of further ionizations that the secondary electron can cause depends on the kinetic energy of the secondary electron, the binding energies of the electrons in the medium are explicitly considered, in contrast to the work of ref 44 (where the effect was less important due to the different treatment of low-energy losses). An energy transfer E' from the primary electron to an electron with binding energy I produces a secondary electron with kinetic energy $E' - I$. The ion escape yield corresponding to such an event is $G_{esc}(E' - I)$; i.e., the yield from a track of an electron with initial energy $E' - I$. The primary electron energy reduces to $E - E'$, and the remaining contribution to the yield of the primary electron is $G_{esc}(E - E')$. Taking all possible energy losses into consideration gives[44]

$$EG_{esc}(\mathrm{E}) = \int_{I_{min}}^{I_{max}}\{\int_{I}^{E/2}[(E' - I)\, G_{esc}(E' - I) + (E - E')\, G_{esc}(E - E')]P(E,E',I)\, \mathrm{d}E'\}\, \mathrm{d}I \quad (3)$$

Note that the method described in this section, which is based on eq 3, holds for any product yield and not only for the ion escape yield.

In eq 3, $P(E,E',I)\, \mathrm{d}E'\, \mathrm{d}I$ is the probability that the incoming electron loses an energy between E' and $E' + \mathrm{d}E'$ to an electron with binding energy between I and $I + \mathrm{d}I$. Following the work of Magee and Chatterjee,[44] eq 3 can, to a good approximation, be used to obtain the derivative of the yield

$$\frac{\mathrm{d}G_{esc}(\mathrm{E})}{\mathrm{d}E} = -\frac{G_{esc}(\mathrm{E})}{E} + \frac{1}{E}\frac{\int_{I_{min}}^{I_{max}}\{\int_{I}^{E/2}(E' - I)\, G_{esc}(E' - I)\, P(E,E',I)\, \mathrm{d}E'\}\, \mathrm{d}I}{\int_{I_{min}}^{I_{max}}\{\int_{I}^{E/2}E'P(E,E',I)\, \mathrm{d}E'\}\, \mathrm{d}I} \quad (4)$$

The probability $P(E,E',I)\, \mathrm{d}E'\, \mathrm{d}I$ is given by

$$P(E,E',I)\, \mathrm{d}E'\, \mathrm{d}I = N^{-1}\left[n(I)\frac{\mathrm{d}\sigma(\mathrm{E},\mathrm{E}')}{\mathrm{d}E'}\right]\mathrm{d}E'\, \mathrm{d}I \quad (5a)$$

with the normalization factor $N = \int\int n(I)(\mathrm{d}\sigma(E,E')/\mathrm{d}E')\, \mathrm{d}E'\, \mathrm{d}I$ and $\mathrm{d}\sigma(E,E')/\mathrm{d}E'$ is the differential cross section for energy loss E' by the primary electron to an electron with binding energy I.

The electron density can, according to the model of section II.A, be written as

$$n(I) = n_v\frac{3}{2}E_F^{-3/2}\sqrt{E_F - 1} + n_c\delta(E_c - I) \quad (5b)$$

The first term in the right-hand side of eq 5b corresponds to the valence electron density (and only appears for $I < E_F$), and the second term containing the Dirac δ function brings the contribution due to the inner-shell electrons with binding energy E_c into account. If the yield $G_{esc}(E)$ up to some energy E is known, the yield at higher energies can be calculated by integration of eq 4, provided that the energy losses by the primary electron are sufficiently separated in space.

For primary electron energies in the MeV range, relativistic effects cannot be neglected, and therefore, relativistic cross sections must be used for $\mathrm{d}\sigma(E,E')/\mathrm{d}E'$ in eq 5a. For excitation of the valence electrons involving energy losses $E' \ll E$, the relativistic Bethe cross section was used. The relativistic Bethe cross section can be written as a sum of a nonrelativistic and a relativistic contribution[29,45]

$$\frac{\mathrm{d}\sigma(E,E')}{\mathrm{d}E'} = \frac{\mathrm{d}\sigma_{NR}(E,E')}{\mathrm{d}E'} + \frac{\mathrm{d}\sigma_{RC}(E,E')}{\mathrm{d}E'} \quad (6a)$$

with the nonrelativistic cross section

$$\frac{\mathrm{d}\sigma_{NR}(E,E')}{\mathrm{d}E'} = \frac{2\pi e^4}{(4\pi\epsilon_0)^2 m_e v^2 E'}\int_{q_-}^{q_+}\frac{\mathrm{d}f(q,E')}{\mathrm{d}E'}\frac{\mathrm{d}q^2}{q^2} \quad (6b)$$

and the relativistic correction term

$$\frac{\mathrm{d}\sigma_{RC}(E,E')}{\mathrm{d}E'} = \frac{2\pi e^4}{(4\pi\epsilon_0)^2 m_e v^2 E'}\frac{\mathrm{d}f(q{=}0,E')}{\mathrm{d}E'}[-(\ln(1 - \beta^2)) - \beta^2] \quad (6c)$$

with v being the velocity of the primary electron and $\beta = v/c$, where c is the speed of light. The minimum and maximum relativistic momentum transfers in eq 6b are equal to

$$q_\pm = \sqrt{2m_eE\left[1 + \frac{E}{2m_ec^2}\right]} \pm \sqrt{2m_eE\left[1 + \frac{E}{2m_ec^2}\right] - 2m_eE'\left[1 + \frac{E}{m_ec^2}\right] + \frac{(E')^2}{c^2}}$$

The generalized oscillator strength $\mathrm{d}f(q,E')/\mathrm{d}E'$ in eqs 6b and 6c was obtained from the energy-loss function $\mathrm{Im}\{-1/\epsilon(q,E')\}$ by using the relation[22,23]

$$\frac{\mathrm{d}f(q,E')}{\mathrm{d}E'} = \frac{8\pi\epsilon_0 m_e E'}{h^2e^2n_v}\mathrm{Im}\{-1/\epsilon(q,E')\} \quad (7)$$

where h is the constant of Planck. The energy-loss function was taken to be equal to that used in the track structure calculations, see section II.A.

For energy losses by the primary electron that are large in comparison to the binding energy of the electrons in the medium but are small compared with the energy of the primary electron, the Bethe cross section is approximately equal to the Møller cross section.[30] For larger energy losses that become comparable to the energy of the primary electron, the Bethe theory is no longer valid and the Møller cross section must be used. For the valence electrons in polyethylene, the Bethe cross section, obtained with the energy-loss function described above, was found to be approximately equal to the Møller cross section for energy losses near 800 eV. Therefore, the Møller cross section was used for $\mathrm{d}\sigma(E,E')/\mathrm{d}E'$ in eq 5a for energy losses, E', above 800 eV. The Møller cross section was also used to describe the excitation of the inner-shell electrons.

For energies of the primary electron above 30 keV, a full computer simulation of the motion of the positive ions and electrons in a track, as described in section II.B, is no longer feasible, due to the large number of ions involved. Therefore, the escape yields for primary electron energies above 30 keV were obtained by numerical integration of eq 4, with the values of $G_{esc}(E)$ for $E < 30$ keV taken from the full simulations. The integration over E' and I, in the right-hand side of eq 4, and over q, in eq 6b, was also performed numerically.

The error in the escape yield from MeV electron tracks, due to the fact that overlap of secondary electron tracks cannot be fully neglected near 30 keV, was found to be small, as will be discussed below.

III. Results and Discussion

A. Ion Escape at Zero External Electric Field. The calculated ion escape yields are presented in Figure 1 for different initial distributions of the electron thermalization

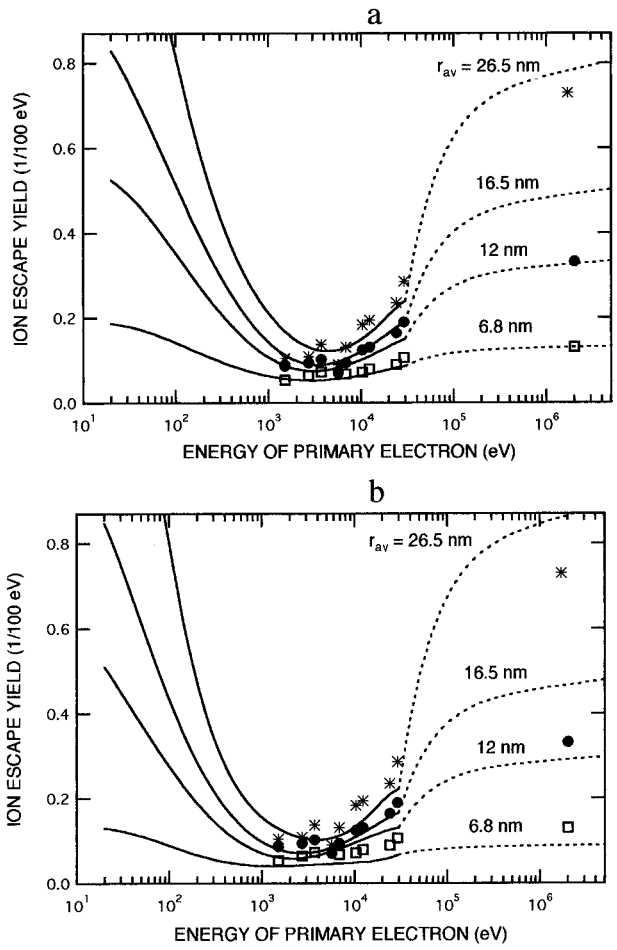

Figure 1. Calculated ion escape yields obtained from full simulations (drawn curves) and by use of the method described in section II.C (dashed curves) for an exponential (a) and a Gaussian electron thermalization distance distribution (b), see eq 1. The experimental results for *n*-hexane (open squares), 2,2,4-TMP (dots), and 2,2,4,4-TMP (asterisks) for primary electron energies were determined from refs 9 and 10. The experimental results in the megaelectronvolt range were taken from refs 7 and 8.

distance, together with experimental results for three hydrocarbon liquids from the literature.[7−10] The drawn parts of the curves for primary electron energies up to 30 keV represent the results of the full simulations described in section II.B. (The curves are an interpolation through the calculated escape yields for a single ion pair (represented at $E = 20$ eV) and 14 different primary electron energies from 40 eV up to 30 keV.) The dashed parts of the curves above 30 keV were obtained by application of the method described in section II.C.

In Figure 1, the calculated ion escape yield is seen to vary dramatically with the energy of the primary electron. The ion escape yield from tracks of electrons with an energy of a few kiloelectronvolts to a few tens of kiloelectronvolts is very much smaller than the ion escape yield for a single ion pair ($E = 20$ eV). For primary electron energies above several tens of kiloelectronvolts, the ion escape yield increases due to a relatively larger contribution of small groups of ions that can be considered as (almost) isolated and that have larger yields than the tracks in the kiloelectronvolt region. It is seen that even in the megaelectronvolt range, the escape yield remains lower than that for a single ion pair.

Figure 1 shows that the general behavior of the calculated curves is in agreement with the experimental results. The experimental values in the kiloelectronvolt region were obtained from the escape yields measured by Holroyd et al. as a function of an external electric field.[9,10] In order to extract the yield at zero external field from these data, the effect of an external field on the ion escape yield was investigated, as will be discussed in section III.B. It is seen that there is considerable scatter in the experimental data. The results for photoelectrons produced by X-rays with energies from 1.8 to 4 keV have been obtained with a different experimental setup than that used for energies and from 5.9 to 29.2 keV. In Figure 1, the escape yields are presented at the energies of the photoelectrons, which are assumed to be 285 eV (the binding energy of a carbon 1s electron) smaller than the X-ray energies. The results in the megaelectronvolt range have been obtained with the Bremsstrahlung from high-energy electrons. The escape yields are plotted at the energies of these electrons, which is in fact the upper limit of the energy of the Bremsstrahlung. Despite the uncertainty in the energy of the initial electrons, however, the calculated results appear to be somewhat higher than the experimental ones. This will be discussed further below.

It should be noted that the calculated escape yields for primary electron energies below 100 eV are somewhat uncertain. The cross section of Ashley et al.[20,21] (which is analogous to the Bethe cross section[29,45]) used to describe the inelastic electron scattering in the track structure calculations is only valid for primary electrons with an energy which is large in comparison to the binding energies of the electrons in the medium. For primary electron energies below 100 eV, the cross section used is less accurate and the calculated track structures for these energies (and, consequently, the escape yields) could be in error.

The binding energies of the valence electrons are not precisely known, and the validity of the description in terms of the free electron model is uncertain. Also, the ionization threshold of the molecules in the medium is not well-defined. It is, therefore, not precisely known to which extent an energy loss by an incoming electron causes an ionization. Therefore, the initial ion yield is uncertain (see also section II.A). As will be discussed below, this uncertainty has only a minor effect on the ion escape yields from tracks of electrons with energies between 100 eV and 30 keV.

The results in Figure 1 were obtained by taking the minimum energy above the Fermi level, to which excitation of an electron must occur in order to give an ion pair, equal to 3.2 eV. This gave an initial ion yield $G_0 = 5.0(100\text{ eV})^{-1}$ within 4% for all primary electron energies between 100 eV and 30 keV. In order to study the effect of the uncertainty in the initial ion yield, G_0, on the escape yield, G_{esc}, calculations were also performed with $G_0 = 5.9(100\text{ eV})^{-1}$. The latter value was obtained if all excitations of the electrons in polyethylene were considered as an ionization. The calculations with $G_0 = 5.9(100\text{ eV})^{-1}$ were performed for a Gaussian electron thermalization distribution with $r_{av} = 6.8$ nm and $r_{av} = 12$ nm, respectively. The calculated escape yields were found to be less than 5% different from those obtained with $G_0 = 5.0(100\text{ eV})^{-1}$ for all primary electron energies between 100 eV and 30 keV. This may be explained in the following way. For the larger initial ion yield, G_0, the density of the ions in the track is larger and the escape probability $p_{esc} = G_{esc}/G_0$ is smaller. However, the decrease of p_{esc} is compensated by the increase of G_0, such that the ion escape yield, $G_{esc} = p_{esc}G_0$, is negligibly affected. The ion escape yield is thus found not to depend appreciably on the initial ion yield for this energy region. For lower energies, this is no longer true, and as will be discussed below, the uncertainty in the yield at low primary electron energy introduces an uncertainty in the yield from megaelectronvolt electron tracks.

Above 30 keV, the large number of ions in the track makes a full simulation of the ion escape no longer feasible, and

therefore, the method of section II.C was used to obtain the escape yields at higher energies. The gradients of the calculated curves in Figure 1 exhibit a discontinuity at 30 keV. The discontinuity indicates that at 30 keV, the energy losses by the primary electron do not yet occur at positions sufficiently separated from each other, such that they can be treated as independent. In order to obtain insight into the error made, the method of section II.C was also applied from a primary electron energy of 20 keV, instead of 30 keV, for an exponential electron thermalization distribution with $r_{av} = 26.5$ nm. Starting the calculation of the escape yield by the method of section II.C from $E = 20$ keV resulted in a 20% larger escape yield around $E = 50$ keV, as compared with that obtained by application of the method of section II.C from 30 keV. At $E = 100$ keV, the difference was reduced to 5% and in the megaelectronvolt range to less than 2%. The calculated values of the escape yield in the megaelectronvolt range are thus not significantly affected by the inaccuracy of the results between 30 and 100 keV. The small effect on the escape yield in the megaelectronvolt range can be understood, since a 1 MeV electron loses only approximately 7% of its energy by energy losses between 30 and 100 keV.

In Figure 2, the ion escape yield is presented as a function of the average thermalization distance for different energies of the primary electron. Figure 2a clearly shows that the escape yield for a single ion pair differs significantly from the yield from a high-energy electron track. The escape yield from a 1-MeV electron track is seen to be about 40% smaller than the escape yield from a single ion pair, and the escape yield from a 2 keV electron track is about an order of magnitude smaller than that for a single ion pair.

Figure 2b shows that for primary electron energies in the kiloelectronvolt range, an exponential electron distribution gives a larger escape yield than a Gaussian distribution with the same average electron thermalization distance.

If the ion escape yield is known for a given primary electron energy, the average thermalization distance (for a given thermalization distribution) can be determined from plots as presented in Figure 2. Previously, thermalization distances have been determined from experimental escape yields for megaelectronvolt tracks, assuming that these tracks consisted of independent ion pairs only. It can be seen from Figure 2a that use of the curve for single ion pairs rather than that for megaelectronvolt electrons gives a thermalization distance, that can be in error by a factor of 2. This will be considered further in section III.C.

The calculated results in Figure 1 resemble qualitatively the results of ref 17, obtained with model tracks. The calculations of ref 17, however, are uncertain because of several approximations. In ref 17, cylindrical tracks were used with average track lengths obtained from range-energy data in water, while in this work the curvature of the track was taken into consideration and the range distribution is explicitly taken into account.

In the work of ref 17, the ion escape yield from tracks of electrons with higher energies was obtained by integration of the derivative of the yield, analogous to the method of section II.C. However, in contrast to the present work, a division was made between energy losses below and above 100 eV, as was also done by Magee and Chatterjee.[44] In ref 17, a distribution of the number of ion pairs in groups, due to energy losses below 100 eV, was taken from experimental work on the gas phase. Unfortunately, the group size distributions in the tracks for $E < 100$ eV from this work are not known accurately. The effect of the group size distribution on the escape yields in the high-energy region was investigated by calculating the escape yields

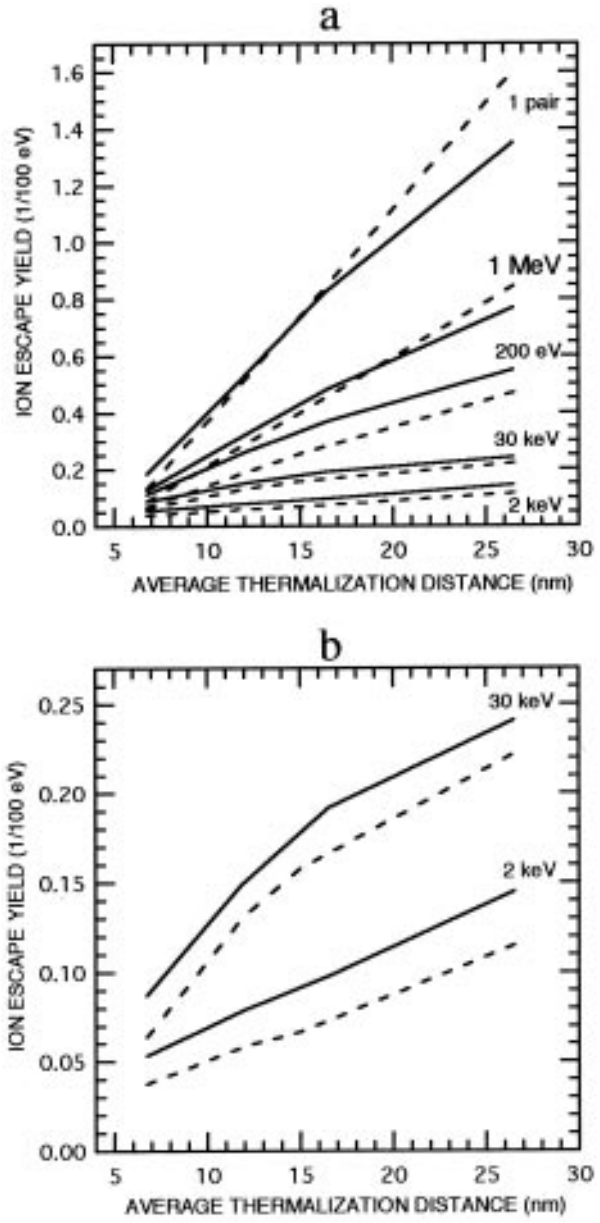

Figure 2. Calculated ion escape yields as a function of the average electron thermalization distance for an exponential (drawn curves) and a Gaussian electron thermalization distribution (dashed curves), see eq 1, for several primary electron energies. The curves connect the calculated escape yields for $r_{av} = 6.8$, 12, 16.5, and 26.5 nm.

for two different group size distributions by the method of ref 17 and comparing the results with those from the full track calculations.

Calculations were performed for a Gaussian electron thermalization distance distribution with $r_{av} = 12$ nm. The frequency distribution, f_N, of the number of ion pairs per group for $N = 1-4$, used in ref 17, was taken ($f_1 = 0.428$, $f_2 = 0.276$, $f_3 = 0.186$, and $f_4 = 0.110$) and compared with a distribution with a much smaller contribution of single pairs ($f_1 = 0.28$, $f_2 = 0.27$, $f_3 = 0.23$, $f_4 = 0.22$). The escape yields for the different group sizes ($N = 1-4$) were obtained from the present results for energies $E = 20$, 40, 60, and 80 eV (corresponding to an initial yield of $G_0 = 5(100\ \text{eV})^{-1}$). These escape yields are within 2% of the yields presented in ref 17 for the corresponding number of ion pairs. This once more shows that the exact initial spatial distribution of the ionizations in the small groups is not critical, which is due to the large Coulomb repulsion at early times that destroys the initial configuration. In both calculations,

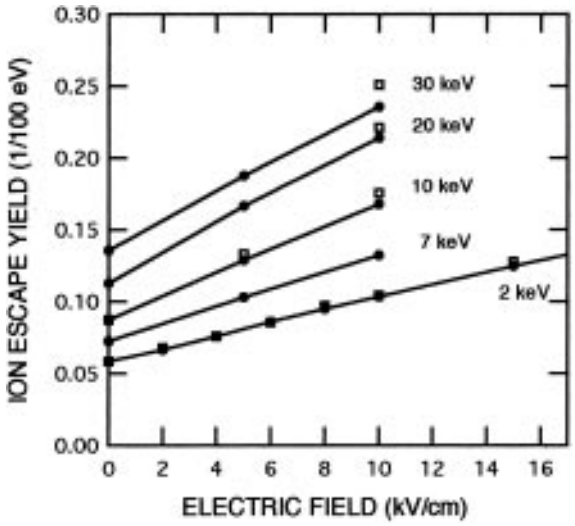

Figure 3. Calculated ion escape yields as a function of the external electric field for several energies of the primary electron. The dots are the results for an external field parallel to the initial direction of motion of the primary electron, and the open squares are for a perpendicular orientation of the field.

the ion escape yields of the present work were taken for energy losses between 100 eV and 30 keV.

For the distribution used in ref 17, a 10% larger escape yield is found in the high-energy region, as compared to the present results from the full track calculations. For the frequency distribution with the smaller contribution of the single pairs, the results were found to be equal to the full track results. It is seen that a rather substantial shift in the group size distribution has only a relatively modest effect on the yields in the high-energy region.

While the results in the kiloelectronvolt region are relatively insensitive to the detailed assumptions about the low-energy events, the results in the high-energy region are affected by the yields due to the low-energy losses. Sufficiently accurate experimental results in the kiloelectronvolt range give information on the thermalization distance distributions. Once these have been determined, comparison of calculated and experimental results in the high-energy region may give information about the ionization processes at low energies.

B. Ion Escape in the Presence of an External Electric Field. As mentioned above, the experimental results for primary electron energies in the kiloelectronvolt range were obtained from literature data on the ion escape yield in the presence of an external electric field.[9,10] Therefore calculations were performed to obtain insight into the dependence of the ion escape yield on both the strength of an external electric field and the orientation with respect to the initial direction of motion of the primary electron. The effect of the orientation of the field was considered, since the high-energy electrons in the experiments of refs 9 and 10 can have a preferred initial direction of motion, due to their production by X-ray photoionization. The angular distribution of photoelectrons is in general not isotropic and is determined by the orientation of the polarization vector of the incident light. In the experiments of refs 9 and 10, the X-ray beam was oriented perpendicular and parallel to the external field, respectively. If the orientation of the X-ray polarization vector with respect to the external field was also different in the experiments of refs 9 and 10, the distribution of the initial direction of motion of the primary electrons with respect to the external field will not be the same in these two experimental studies.

In the calculations, electron tracks were used, without scaling of the coordinates of the positive ions for the correction due to the density difference between polyethylene and the hydrocarbon liquids. All excitations of electrons above the Fermi level were considered to be ionizations, giving $G_0 = 5.9(100\ \text{eV})^{-1}$. The electron thermalization distribution was taken as a Gaussian with $r_{av} = 12$ nm.

TABLE 1: Average Thermalization Distances, r_{av}, Obtained from a Comparison of the Calculated and Experimental Ion Escape Yields for Primary Electron Energies between 1.5 and 28.9 keV

		r_{av} (nm)
n-hexane	exptl	8 ± 1
	Gauss	10 ± 1
2,2,4-TMP	exptl	15 ± 2
	Gauss	20 ± 3
2,2,4,4-TMP	exptl	>22
	Gauss	>26

The calculated results in Figure 3 show that, for the field strengths considered, the ion escape yield from electron tracks increases linearly with the field strength. This has also been predicted for low fields by Tachiya and Hummel.[40] For single ionizations, the linear increase of the ion escape probability at low external electric fields is a well-known result of the Onsager theory.[37] According to the Onsager theory, the slope-to-intercept ratio of the escape yield as a function of the electric field strength is equal to $e^3/(8\pi\epsilon_0\epsilon_r kT)$. For an external electric field parallel to the initial direction of motion of the primary electron, the slope-to-intercept ratio of the lines increases from 0.079 cm/kV for a primary electron energy of 2 keV to 0.093 cm/kV for 10 keV and then decreases to 0.073 cm/kV for 30 keV. These values are larger than the slope to intercept ratio for a single ion pair, which according to the Onsager theory equals 0.055 cm/kV for $\epsilon_r = 2$.

The yield is not seen to differ very much for fields parallel or perpendicular to the initial direction of motion of the primary electron. For a primary electron energy of 2 keV, the track structure is not very straight, and therefore, it is not surprising that the escape yield is equal for fields parallel and perpendicular to the initial direction of motion of the primary electron. At higher primary electron energies, the track structure becomes more straight and the orientation of the field is seen to have some effect on the ion escape yield.

On the basis of the observed linear increase of the calculated ion escape yield with external field strength, the experimental yields at zero field in Figure 1 were determined by linear extrapolation of the yields in refs 9 and 10 to zero field.

C. Thermalization Distance Distribution. The results for primary electron energies up to 30 keV will be considered first. The experimental results for primary electron energies below 30 keV were obtained from a linear extrapolation to zero external field strength of the experimental data of Holroyd et al.,[9,10] as discussed above. The escape yields for *n*-hexane, 2,2,4-TMP (2,2,4-trimethylpentane), and 2,2,4,4-TMP (2,2,4,4-tetramethylpentane) are given in Figure 1. For all three hydrocarbon liquids, the experimental yields exhibit a discontinuity on going from a primary electron energy of 3.7 keV to higher energy. This discontinuity could be due to the fact that the yields below 3.7 keV from ref 10 were measured with another experimental setup than used to measure the yields at higher energies in the work of ref 9. The average thermalization distances, r_{av}, for these liquids were obtained by drawing a smooth curve through the experimental data and taking the yields at 2, 10, and 30 keV to obtain the r_{av} value from plots as shown in Figure 2 (the plots for 10 keV are not shown in Figure 2). The results are presented in Table 1. The uncertainty in the values of r_{av} in Table 1 is due to the scatter in the

experimental data. An exponential distribution gives smaller average thermalization distances than a Gaussian distribution.

The experimental results plotted at megaelectronvolt energies in Figure 1 were taken from refs 7 and 8. In the experiments of refs 7 and 8, a Bremsstrahlung produced with megaelectronvolt electrons was used. The experimental results in Figure 1 are plotted at the energy of these megaelectronvolt electrons. However, in the experiments, the primary electrons result from Compton scattering of Bremsstrahlung, which has a broad energy distribution.[46] By considering the energy distribution of the primary electrons and realizing that the escape yield does not change by more than 20% for energies between 0.1 and 2 MeV (see Figure 1), it was concluded that this effect could account for an error of less than 10% in the yield.

In the experimental work of refs 7 and 8, electron thermalization distance distributions were determined from the yield of escaped ions from tracks of electrons with energies in the megaelectronvolt range. The most probable thermalization distance for a Gaussian distribution, b_G, as reported in ref 7, is related to the average thermalization distance according to $r_{av} = 2b_G/\sqrt{\pi}$. The values of r_{av} for *n*-hexane and 2,2,4-TMP found from ref 7 are 7.6 and 10.7 nm, respectively. For the relatively large escape probability as found for 2,2,4,4-TMP,[8] the dispersion parameter, b_{GP}, in the Gaussian-power distribution used in ref 8, is approximately equal to b_G.[47] It is then found from the reported value of b_{GP} in ref 8 that the average thermalization distance for 2,2,4,4-TMP is larger than 14.8 nm. In the work of refs 7 and 8, the ion escape yield is described by using the Onsager formula for single ion pairs,[37] with the gas-phase value for the initial ion yield,[7] or assuming $G_0 = 4.4(100\ \text{eV})^{-1}$.[8] The values of r_{av} found from the work in refs 7 and 8 are considerably smaller than those for a Gaussian distribution in Table 1. As was observed above, the determination of the thermalization distances from experimental escape yields for megaelectronvolt tracks, using the single pair treatment, is unsatisfactory. In addition, in this treatment, a value for the total yield of ion pairs has to be assumed, which introduces another uncertainty.

D. Ion Escape Yield for Small Energy Losses. Assuming that the values of r_{av} in Table 1, as found from the data in the kiloelectronvolt range, are correct, the calculated escape yields in the megaelectronvolt range are found to be larger than the experimental values. For *n*-hexane and 2,2,4-TMP, the ion escape yields in the megaelectronvolt range, calculated with an exponential thermalization distance distribution and the values of r_{av} from Table 1, are approximately 25% larger than the experimental values from ref 7. This difference exceeds the experimental error, which is estimated to be less than 10%. Figure 1a shows that for 2,2,4,4-TMP, the calculated ion escape yields for an exponential thermalization distribution with $r_{av} \sim 26$ nm are close to the experimental values in the kiloelectronvolt range. The escape yield calculated with this thermalization distance distribution is less than 10% larger than the experimental value for 2,2,4,4-TMP in the megaelectronvolt range from ref 8 and does not exceed the experimental error.

The calculated ion escape yields in the megaelectronvolt range, obtained with a Gaussian electron thermalization distance distribution and the r_{av} values from Table 1, are approximately 50% larger than the experimental values for *n*-hexane and 2,2,4-TMP. For 2,2,4,4-TMP, the escape yield in the megaelectronvolt range, calculated for a Gaussian thermalization distance distribution with $r_{av} \sim 26$ nm, is approximately 15% larger than the experimental value.

The escape yield from high-energy electron tracks is determined by the energy loss probability distribution, $P(E,E',I)$, and by the escape yield, $G_{esc}(E' - I)$, from tracks of secondary electrons with energy $E' - I$, as can be seen in eqs 3 and 4. Inaccuracies in $P(E,E',I)$ as well as in $G_{esc}(E' - I)$ will thus be reflected in an inaccuracy in the yield from high-energy electron tracks, as obtained by the method of section II.C.

The energy-loss probability distribution, $P(E,E',I)$, as given in eq 5a, was calculated by use of the Bethe cross section in eq 6 and the electron density in eq 5b. The Bethe cross section was obtained by using the optical oscillator strength for polyethylene from ref 25, which does not differ substantially from that of the hydrocarbon liquids of interest, as was discussed in section II.A. Therefore, it is considered unlikely that the overestimation of the calculated escape yields from megaelectronvolt electron tracks is due to an inaccuracy in the calculated Bethe cross section. The valence electrons in the medium were described as a free electron gas, giving binding energies, I, of the electrons between 0 eV and $E_F = 13.8$ eV, with a maximum density of electrons with zero binding energy; see eq 5b. This model could give an average electron binding energy, which is a few electronvolts smaller than in saturated hydrocarbon liquids, and hence secondary electron energies, $E' - I$, that are somewhat too large. However, as can be seen in Figure 1, an inaccuracy of a few electronvolts in the electron energy does not affect the escape yield very much.

The calculated escape yields at high primary electron energies could be too large due to the fact that the ion escape yields, G_{esc}, at low energies are too large. An inaccuracy at low energies is important, since the escape yield from high-energy electron tracks is relatively sensitive to a variation of the yield at low energies. This is due to the fact that the energy loss probability function, $P(E,E',I)$, has a maximum for losses near $E' = 21$ eV and decreases as the energy loss increases. Also, the escape yield from low energy electron tracks is much larger than at kiloelectronvolt energies, which once more causes the yield at high energies to be sensitive to that at low energies.

As was discussed in section III.A, the escape yields at low energies are rather uncertain. The inelastic scattering cross section used to calculate the initial track structures is not appropriate for electrons with energies below 100 eV. Also, the approximate description of the binding energies of the valence electrons by the free electron model introduces an uncertainty in the energies of the secondary electrons ejected. Furthermore, the energy above which ionization occurs is not known. These uncertainties introduce an inaccuracy in the inital ion yields and, hence, in the escape yields. However, it was shown that variation of the initial yield of ionization between $G_0 = 5(100\ \text{eV})^{-1}$ and $G_0 = 5.9(100\ \text{eV})^{-1}$ had only a minor effect on the ion escape yield for primary electron energies in the region from 100 eV to 30 keV. For smaller energies, the effect of the initial ionization yield on the yield of escape becomes increasingly larger.

It was found that a reduction of the ion escape yield for energies below 100 eV by approximately 25% brings the calculated and experimental results in the megaelectronvolt range into agreement, if an exponential electron thermalization distribution is used. For a Gaussian electron thermalization distribution, a reduction by 50% is needed. The discrepancy between the calculated and experimental ion escape yields from megaelectronvolt electron tracks indicates that the initial yield of ionization in the liquids considered is lower than 5 $(100\ \text{eV})^{-1}$. From the yields of electron scavenging at high scavenger concentrations in cyclohexane,[48] *cis*- and *trans*-decalin,[49] and 2,2,4-TMP,[50] it is concluded that the initial yield of ionization is not smaller than about $4(100\ \text{eV})^{-1}$. This would indicate that the form of the electron thermalization distribution is

exponential rather than Gaussian, since in order to explain the results in the megaelectronvolt region for an exponential an initial ion yield of about $4(100\ \text{eV})^{-1}$ is needed, while for a Gaussian distribution this is considerably lower. Computer simulations of the electron scavenging are currently carried out in order to further substantiate this conclusion.

IV. Summary and Conclusions

The ion escape yield from high-energy electron tracks in saturated hydrocarbon liquids was calculated by means of computer simulations and compared with experimental results from the literature. The initial track structures were calculated by using the scattering characteristics of an electron in polyethylene, which was considered to be representative of saturated hydrocarbon liquids. For tracks of electrons with an energy up to 30 keV, the yield of escaped ions was obtained by a computer simulation of the motion of the positive ions and electrons. The ion escape yield from tracks of electrons with energies above 30 keV was obtained from the ion escape yields at lower energies.

The calculated ion escape yields exhibit a large variation as a function of the energy of the primary electron. The escape yield from high-energy electron tracks is significantly different from the yield for a single ion pair with the same electron thermalization distribution. Average electron thermalization distances were obtained by comparing the calculated ion escape yields with experimental values of the escape yield from tracks of electrons with energies between 1.5 and 30 keV. Information about the initial number of ionizations and the shape of the electron thermalization distribution was obtained by comparing calculated and experimental ion escape yields from megaelectronvolt electron tracks.

The ion escape yield from electron tracks with energies from 2 up to 30 keV was found to increase linearly with the strength of an external field up to 15 kV/cm. The difference in the escape yields for a parallel or perpendicular orientation of the electric field, with respect to the direction of motion of the primary electron, was found to be negligible.

References and Notes

(1) *Kinetics of Nonhomogeneous Processes*; Freeman, G. R., Ed.; Wiley: New York, 1987; Chapters 2−6.
(2) *Radiation Chemistry Principles and Applications*; Farhataziz; Rodgers, M. A. J., Ed.; VCH: New York, 1987.
(3) Rice, S. A. In *Chemical Kinetics*; Bamford, C. H.; Tipper, C. F. H.; Compton, R. G., Eds.; Elsevier: Amsterdam, 1985.
(4) Hummel, A. *Can. J. Phys.* **1990**, *68*, 858.
(5) Brocklehurst, B. *J. Chem. Soc., Faraday Trans.* **1992**, *88*, 167.
(6) Brocklehurst, B. *J. Chem. Soc., Faraday Trans.* **1992**, *88*, 2823.
(7) Schmidt, W. F.; Allen, A. O. *J. Chem. Phys.* **1970**, *52*, 2345.
(8) Ryan, T. G.; Freeman, G. R. *J. Chem. Phys.* **1978**, *50*, 5144.
(9) Holroyd, R. A.; Sham, T. K. *J. Phys. Chem.* **1985**, *89*, 2909.
(10) Holroyd, R. A.; Sham, T. K.; Yang, B. X.; Feng, X. H. *J. Phys. Chem.* **1992**, *96*, 7438.
(11) Clifford, P.; Green, N. J. B.; Pilling, M. J. *J. Phys. Chem.* **1982**, *86*, 1318.
(12) Clifford, P.; Green, N. J. B.; Pilling, M. J. *J. Phys. Chem.* **1987**, *91*, 4417.
(13) Green, N. J. B.; Pilling, M. J.; Pimblott, S. M.; Clifford, P. *J. Phys. Chem.* **1989**, *93*, 8025.
(14) Green, N. J. B.; Pimblott, S. M. *J. Phys. Chem.* **1990**, *94*, 2922.
(15) Green, N. J. B.; Pimblott, S. M. *J. Chem. Soc., Faraday Trans.* **1993**, *89*, 1299.
(16) Pimblott, S. M.; Green, N. J. B. *Rad. Phys. Chem.* **1996**, *47*, 233.
(17) Bartczak, W. M.; Hummel, A. *J. Phys. Chem.* **1993**, *97*, 1253.
(18) Bartczak, W. M.; Hummel, A. *J. Chem. Phys.* **1987**, *87*, 5222.
(19) Terrissol, M. *Methode de simulation du transport d'electrons d'energies comprises entre 10 eV et 30 keV*. Thesis, Université de Paul Sabatier de Toulouse, 1978.
(20) Ashley, J. C.; Cowan, J. J.; Ritchie, R. H.; Anderson, V. E.; Hoelzl, J. *Thin Solid Films* **1979**, *60*, 361.
(21) Ashley, J. C. *J. Electron. Spectrom. Rel. Phenom.* **1982**, *28*, 177.
(22) Fano, U.; Cooper, J. W. *Rev. Mod. Phys.* **1968**, *40*, 441.
(23) *Microdosimetry and Its Applications*; Rossi, H. H., Zaider, M., Eds.; Springer: Berlin, 1996.
(24) LaVerne, J. A.; Pimblott, S. M. *J. Phys. Chem.* **1995**, *99*, 10540.
(25) Painter, L. R.; Arakawa, E. T.; Williams, M. W.; Ashley, J. C. *Rad. Res.* **1980**, *83*, 1.
(26) Ritchie, R. H. *Phys. Rev.* **1959**, *114*, 644.
(27) Gryzinsky, M. *Phys. Rev. A* **1965**, *138*, 336.
(28) Mott, N. F. *Proc. R. Soc. London* **1930**, *A126*, 259.
(29) Inokuti, M. *Rev. Mod. Phys.* **1971**, *43*, 297.
(30) Moller, C. *Ann. Phys.* **1932**, *14*, 531.
(31) Scofield, J. H. In *Atomic Inner Shell Processes*; Craseman, B., Ed.; Academic: 1973.
(32) *Electronic and Ionic Impact Phenomena II*; Massey, H. S. W., Ed.; Clarendon: Oxford, 1969.
(33) Cox, H. L.; Bonham, R. A. *J. Chem. Phys.* **1967**, *47*, 2599.
(34) *Solid State Physics*; Ashcroft, N. W.; Mermin, N. D., Eds.; Holt-Saunders International Editions: 1979.
(35) Adler, P.; Bothe, H. K. *Z. Naturforsch.* **1965**, *20a*, 1700.
(36) Hummel, A. In *The Chemistry of Alkanes and Cycloalkanes*; Patai, S., Rappoport, Z., Eds.; Wiley: New York, 1992.
(37) Onsager, L. *Phys. Rev.* **1938**, *54*, 554.
(38) Takayasu, H. *J. Phys. Soc. Jpn.* **1982**, *51*, 3057.
(39) Tachiya, M. *J. Chem. Phys.* **1988**, *89*, 6929.
(40) Tachiya, M.; Hummel, A. *Chem. Phys. Lett.* **1989**, *154*, 497.
(41) Sceats, M. G. *J. Chem. Phys.* **1989**, *90*, 2666.
(42) Mozumder, A. *J. Chem. Phys.* **1990**, *92*, 1015.
(43) Bartczak, W. M.; Hummel, A. Preliminary results.
(44) Magee, J. L.; Chatterjee, A. *J. Phys. Chem.* **1978**, *82*, 2219.
(45) Bethe, H. In *Handbuch der Physik*; Geiger, H., Scheel, K., Eds.; Springer: Berlin, 1933.
(46) *The Quantum Theory of Radiation*; Heitler, W., Ed.; Clarendon: Oxford, 1954.
(47) Freeman, G. R. In *Kinetics of Nonhomogeneous Processes*; Freeman, G. R., Ed.; Wiley: New York, 1987.
(48) Warman, J. M.; Asmus, K. D.; Schuler, R. H. *J. Phys. Chem.* **1969**, *73*, 931.
(49) Hummel, A. Unpublished results.
(50) Rzad, S. J.; Bansal, K. M. *J. Phys. Chem.* **1972**, *76*, 2374.